iTRAQ-based quantitative proteomic analyses the cycle chronic heat stress affecting liver proteome in yellow-feather chickens

Quan Zhang,*[,1,2] YuZe Yang,†[,1] YongQiang Lu,† and ZiWen Cao*

*College of Coastal Agricultural Sciences, Guangdong Ocean University, Zhanjiang, China; and †Beijing General Station of Animal Husbandry, Beijing, China

ABSTRACT Heat stress (**HS**) is one of the main environmental factors affecting the efficiency of poultry production. The yellow-feather chickens (**YFC**) as an indigenous strain of chicken is a popular poultry breed in China. Our previous study used the RNA-seq to analyze the gene expression profiles of male YFC under HS and showed that the lipid and energy metabolism pathways are activated in livers of YFC exposed to acute HS (38°C, 4 h and 25°C recovery 2 h). In this study, we used quantitative proteome analysis based on iTRAQ to study the liver response of YFC to cycle chronic HS (38 ± 1°C, 8 h/d, 7 d, **CyCHS**). The male YFCs treatment used the CyCHS from 22 to 28 days of age. The liver tissue samples were collected at 28 d old. A total of 39,327 unique peptides matches were detected using iTRAQ analysis and 4,571 proteins exhibited a false discovery rate of 1% or less. Forty-six significant differentially expressed proteins (**DEPs**) were detected in the CyCHS group compared with the control group for the liver samples, including up- and down-regulated DEPs were 18 and 28, respectively. We found that the enriched biological process terms of the DEPs expressed in the liver were related to DNA metabolic process, oxidation-reduction process, oxidative stress and gluconeogenesis. In KEGG pathway analysis. Most of the hepatic DEPs were annotated to glutathione metabolism and TCA cycle in response to CyCHS. The up-regulation of 5 DEPs (GPX1, GSTT1, GSTT1L, RRM2, and LOC100859645) in the glutathione metabolism pathway likely reflects an attempt to deal with oxidative damage by CyCHS. The down-regulation of 3 DEPs (Isocitrate dehydrogenase [**IDH3A**], IDH3B, and phosphoenolpyruvate carboxykinase 1) in the TCA cycle pathway contributes to the regulation mechanism of energy metabolism and probably to cope with the balance of heat production and dissipation during CyCHS in order to adapt to high temperature environments. Our results provide insights into the potential molecular mechanism in heat-induced oxidative stress and energy in YFCs and future studies will investigate the functional genes associated with the response to HS.

Key words: yellow-feather chicken, liver, cycle chronic heat stress, proteome

2021 Poultry Science 100:101111
https://doi.org/10.1016/j.psj.2021.101111

INTRODUCTION

Environmental factors affecting the efficiency of poultry production, especially the ambient temperature. The body weight gain of chickens decreased under the high ambient temperature (Cahaner and Leenstra, 1992; Azad, et al., 2010; Zhang, et al., 2019). The yellow-feather chickens (**YFC**) as an indigenous strain of chicken is a popular poultry breed in China, that is known for its slow-growing and unique meat flavor. Heat stress (**HS**) is known to be less harmful to YFC, especially with respect to weight gain (Azad et al., 2010; Zhang et al., 2019) and the relative weight of tissues (Quinteiro-Filho et al., 2010; Zhang et al., 2017; Zhang et al., 2019).

Investigations into the molecular dynamics of HS adaptation in chickens have made use of a variety of tissues and stress types (Lan et al., 2016; Zhang et al., 2019; Zhang et al., 2020). Multiple cellular pathways are activated in broilers in response to chronic HS, including the endocrine system (Coble et al., 2014), cell cycle regulation, DNA replication (Jastrebski et al., 2017) and the cellular immune response (Tang et al., 2015). Our previous study used the RNA-seq to analyze the gene expression profiles of male YFC under acute HS and showed that the lipid and energy metabolism pathways are activated in livers of YFC exposed to HS (38°C, 4 h and 25°C recovery 2 h) (Zhang et al., 2020) and energy

Received September 15, 2020.
Accepted March 2, 2021.

[1]These authors contributed equally to this work.
[2]Corresponding author: zhang_quan@cau.edu.cn

metabolism progress are involved in heart of YFC under chronic HS (38°C, 8 h/d, 7 d) (Zhang et al., 2019). It's reasonable to hypothesize that the YFC will maintain nutrients metabolism to response HS.

The important function of liver is regulating nutrients metabolism and maintaining homeostasis (Blikslager et al., 2017). Therefore, the liver is an excellent target to study the adaptation mechanism under HS. Proteomic analysis of liver in pekin ducks showed that the pekin ducks coped with HS by regulating amino acid metabolism, cell death and apoptosis and oxidation reduction (Zeng et al., 2013). Proteomic studies on chicken embryonic liver development showed that the development of chicken embryonic liver was related to cell division, carbohydrate metabolism, signal transduction and lipid metabolism (Jianzhen et al., 2007). The result of broiler liver proteomic analysis indicated that the broiler liver involved in extracellular signal-regulated protein kinases (**ERK**) signaling pathway, lipid and amino acid metabolism and cell immune responses to adapt to HS (Tang et al., 2015).

Shotgun proteomics can quantify proteins and provide more detailed description of the interaction mechanism in different species and HS. In this study, we used quantitative proteome analysis based on iTRAQ to study the liver proteomic response of YFCs to HS. The proteomic profiles suggest that DEPs caused by HS are mainly involved in glutathione metabolism and TCA cycle pathway, resulting in the impairment of metabolic function and suggests that the liver of YFCs might activate anti-oxidants response and energy mechanism for dealing with HS, and warrants further insights on the potential mechanisms of HS resistance.

MATERIALS AND METHODS

Animals Treatment and Liver Tissue Samples Collection

Effects of high temperature on the growth of chicken was difference with sex, the reductions in body weight due to HS were much larger in males than in females (Cahaner and Leenstra, 1992). In this study, the male YFCs and experimental house were provided from Guangdong YingFu Agricultural Co., Ltd. (Guangdong, China) on day of hatch. During the experiment, the chickens were provided with *ad libitum* access to water and feed of the same diet which comply with the NRC requirements National Research Council (NRC, 1994). The lighting schedule was 23L (light): 1D (dark). The 18 weight-matched male YFCs were selected at 17 d old and randomly equal assigned in two similar environmentally controlled rooms to acclimate for 5 d. Each room was contented three cages of which $450 \times 300 \times 250$ cm (length × width × height) as 3 biological replicates. Each biological replicate contained three male YFCs. According to the period of high ambient temperature, HS is defined as acute HS (rapid and short rise in ambient temperature) and chronic HS (high ambient temperature over days to weeks). Further, chronic HS is distinguished cyclic chronic HS (a limited time of high temperature consequent by normal temperature for the rest of a day, CyCHS) or constant chronic HS (continuous high ambient temperature, CoCHS) (Akbarian et al., 2016). The CyCHS is extensive used in previous studies (Azad, et al., 2010; Van Goor et al., 2015; Jastrebski et al., 2017; Zhang et al., 2019). In this study, the animal treatment used the CyCHS from 22 to 28 d of age for YFCs. Based on the environment temperature simulation, the temperature in one of the rooms was raised to 38 ± 1°C for 8 h (9:00-17:00) and otherwise maintained at 25 ± 1°C (as the CyCHS group). And another room temperature constant maintained at 25 ± 1°C (as the control group). The relative humidity kept at 50 ± 5% in the control and CyCHS groups. The YFCs were euthanized at 28 d old (17:00) and liver tissue samples were collected, immediately frozen in liquid nitrogen, and stored at −80°C for further use. All YFCs were cared for and treated in accordance with the Guangdong Ocean University Animal Care and Use Committee guidelines (permit number: SYXK 2014-0053).

Total Protein Extraction From Liver Tissue Samples

The 18 liver tissue samples were used for protein extraction. Each sample (0.5 g) was ground in liquid nitrogen and dissolved in 150 μL of lysis buffer (100 mM NH_4HCO_3 (pH 8), 6 M urea and 0.2% SDS) containing 1 mM PMSF and a protease inhibitor cocktail (Cell Signaling Technology, Danvers, MA), followed by 5 min of ultrasonication on ice. The lysate was centrifuged (12000 *g*, 4°C, 15 min) and the cellular debris was removed. The Pierce BCA protein assay kit (Thermo Scientific, USA) was used to measure the concentrations of the extracted proteins according to the manufacturer's instructions (An et al., 2014).

iTRAQ Experiments

For this procedure, Equal-quantity different protein samples from three YFCs in the same biological replicate were mixed to form pooled protein samples as one biological replicate sample. There were 6 pooled protein biological samples (3 biological replicates per group) to proteomic analysis. The pooled protein samples as one biological replicate was used for proteomic analysis in previous studies (Diz, et al., 2009; Luo, et al., 2013; Tang et al., 2015). 120 μg protein sample was taken from each biological sample and the volume was made up to 100 μL with lysis buffer containing 3 μL of 1 μg/μL trypsin and 500 μL of 50 mM TEAB buffer. The samples were digested at 37°C overnight. Each sample was reconstituted in 20 μL of 1 M TEAB buffer and labeled with iTRAQ labeling reagent (control samples: iTRAQ113, iTRAQ114, or iTRAQ115, CyCHS samples: iTRAQ116, iTRAQ117, or iTRAQ118). The labeled samples were mixed with shaking for 2 h at room temperature, and the reaction was stopped by adding 100 μL of 50 mM Tris-HCl (Ph = 8). The labeling samples

were mixed with equal volume, desalted and lyophilized. The lyophilized powder was dissolved in solution 2% acetonitrile (pH10) and centrifuged at 15,000 *g* for 20 min at 4°C. The sample fraction was used on a Rigol L3000 HPLC system by C18 column (Waters BEH C18 4.6 × 250 mm, 5 μm) and the column oven was 50°C. The eluates were collected and dried by vacuum, and reconstituted in formic acid (FA) of 0.1% (v/v) in water. EASY-nLC 1200 UHPLC system (Thermo Fisher, Waltham, MA) coupled with an Q Exactive HF-X mass spectrometer (MS, Thermo Fisher, Waltham, MA) were used in Shotgun proteomics analyses. Sample was put into C18 Nano-Trap column (2 cm × 75 μm, 3 μm). Linear gradient elution was used to peptides separation with an analytical column (15cm × 150μm, 1.9μm). The separated peptides were subjected to Nanospray ionization and analyzed by Q Exactive HF-X MS (Thermo Fisher, Waltham, MA). The top 40 precursors of the highest abundant peptides were selected and fragmented by higher energy collisional dissociation with scan resolution of 60000 and analyzed in MS/MS with a normalized collision energy setting fo 32% and resolution of 15000. The raw data of MS detection have been stored in the ProteomeXchange Consortium via the iProX partner repository with the dataset identifier PXD019971 (http://proteomecentral.proteomexchange.org).

Peptide Identification and Proteins Functional Analysis

The resulting spectra from each fraction were used for individual searches against the UniprotKB database (https://www.uniprot.org/proteomes/UP000000539) using the Proteome Discoverer 2.2 search engine (PD2.2, Thermo Fisher, Waltham, MA). The search parameters were set to identify proteins containing at least 1 unique peptide, with a false discovery rate (**FDR**) of no more than 1.0%. Proteins containing similar peptides that could not be distinguished by MS/MS analysis were identified as belonging to the same protein group. Reporter quantification (iTRAQ 8-plex) was used for iTRAQ quantification. The protein quantification results were statistically analyzed using the Mann-Whitney test and proteins which exhibited significantly different levels between the CyCHS and control groups ($\log_2$ Fold Change > 1.2 or < 0.83 and $P < 0.05$) were defined as differentially expressed proteins (**DEPs**).

The enrichment analysis of Gene Ontology (**GO**) and Kyoto Encyclopedia of Genes and Genomes (**KEGG**) for DEPs in liver tissue were carried out by InterProScan-5 program (Philip et al., 2014) and KEGG database (https://www.kegg.jp), respectively.

Analysis of Selected DEPs by Parallel Reaction Monitoring (PRM) and Real-time PCR (qRT-PCR) Verification

Eight of the 46 DEPs were selected for PRM and qRT-PCR verification: GPX1, IDH3A, HAO2, GSTT1, LOC100859645, ST13P5, HSPH1 and TIMD4. These selected DEPs associated with the enrichment BP or KEGG pathways and heat stress proteins (**HSPs**). The PRM and qRT-PCR was used for proteomic data validation in a number of studies (Ren et al., 2017; Deng et al., 2020; La et al., 2020). Eighteen liver tissues were detected by PRM or qRT-PCR. After reductive alkylation and enzymatic hydrolysis, the purified peptide was dissolved in mass spectrometry buffer (2% acetonitrile, 0.1% formic acid). According to our proteomic results, The Xcalibur 4.0 software (Thermo Fisher, Waltham, MA) was set based on the peptide information suitable for PRM analysis. The HPLC system was used to chromatographic separation and Q-Exactive HF MS (Thermo Fisher, Waltham, MA) was used for PRM/MS. The time of full MS-PRM sepectrometry detection was 90 min. The full MS-PRM scan range was 300-1300 m/z. thirty-one PRM scans were selected based on the inclusion list after each first-order full MS-PRM scan. The raw data of PRM were analyzed by Skyline 3.5.0 (Maclean et al., 2010). To further demonstrate the proteomic data, qRT-PCR was used to measure the gene expression at RNA level. Total RNA of liver tissue samples was isolated according to Qiagen RNeasy Plus Mini Kit (Qiagen, Germantown, MD). RNA quality and quantity were test by agarose gel electrophoresis and spectrophotometer (Nanodrop 2000, Thermo Fisher, Waltham, MA), respectively. And the TransScript RT/RI Enzyme Mix (Transgen Biotech, China) was used to reverse transcription from total RNA to cDNA. The qRT-PCR was

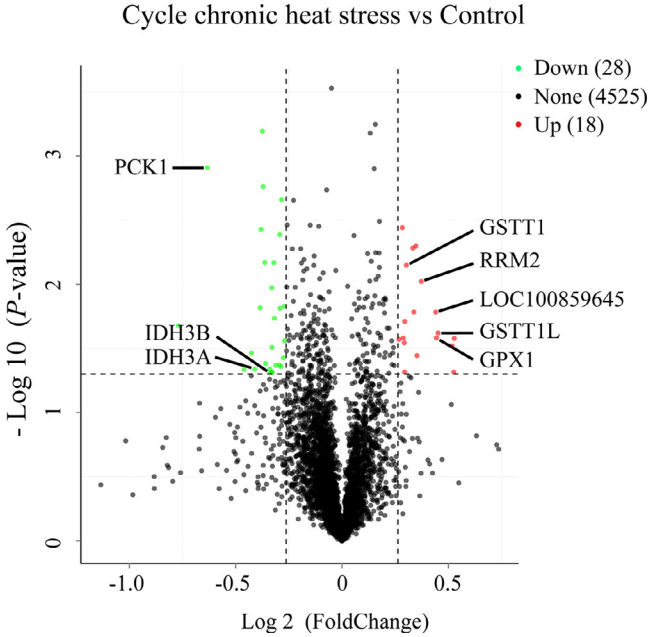

Figure 1. Analysis of differentially abundant proteins. Red, green, and black dots on the graph represent the significantly up-regulated, down-regulated, and unchanged, respectively, between the cycle chronic heat stress and control group. The DEPs, including GPX1, GSTT1, GSTT1L, LOC100859645 and RRM2, enriched in glutathione metabolism KEGG pathway. The DEPs, including IDH3A, IDH3B and PCK1, enriched in citrate cycle KEGG pathway.

performed on the Applied Biosysterms 7500 Fast Real-time PCR System (Thermo Fisher, Waltham, MA) using SYBR Green Real-time PCR Master Mix (Takala, Dalian, China). The qRT-PCR cycling conditions were 95 for 30s, 40 cycles of 95 for 10s and 60 for 30 s. qRT-PCR data were used the $2^{-\Delta\Delta CT}$ method (Livak and Schmittgen, 2001). The primer pairs used are shown in S1 File.

Statistical Analysis

The values obtained for qRT-PCR and PRM were expressed as mean ± SE and analyzed using Statistical Package for the Social Sciences (SPSS) software (v19.0, IBM, USA) by t-test. $P < 0.05$ or 0.01 were considered significant or very significant, respectively.

RESULTS

Identification of Proteomic Data and Differentially Expressed Proteins (DEPs)

A total of 39,327 unique peptides matches were detected using iTRAQ analysis (S2 File) and 4,571 proteins exhibited an FDR of 1% or less (S3 File). The molecular weights (MWs) of most of the proteins and the isoelectric point (pI) values ranged from 20 to 60 kDa and 5 to 9, respectively. The protein sequences with coverage less than 10% accounted for 40%,

Table 1. Statistically significant differentially regulated proteins identified by iTRAQ analysis of liver in yellow-feather chickens under cycle chronic heat stress.

#	Protein name (entry name)	Fold change	Unique peptides	adj. *P* value	Gene name
1	Ig-like domain-containing protein (A0A3Q2UMU2)	0.586	1	0.021	novel gene
2	phosphoenolpyruvate carboxykinase 1 (F1NKP4)	0.644	5	0.001	PCK1
3	ADAM metallopeptidase domain 10 (Q5F3N4)	0.727	5	0.046	ADAM10
4	ladinin 1 (E1C667)	0.744	5	0.034	LAD1
5	isocitrate dehydrogenase 3 (NAD(+)) alpha (A0A1L1RX65)	0.752	10	0.046	IDH3A
6	ubiquitin like 5 (A0A1D5PWV5)	0.766	2	0.015	UBL5
7	PATJ, crumbs cell polarity complex component (A0A1D5P022)	0.768	3	0.004	PATJ
8	T-cell immunoglobulin and mucin domain containing 4 (A0A1L1RJJ0)	0.771	5	0.001	TIMD4
9	hydroxyacid oxidase 2 (E1C0E1)	0.773	7	0.002	HAO2
10	BTB domain-containing protein (A0A1D5PE76)	0.777	1	0.007	novel gene
11	GTP cyclohydrolase I feedback regulator (A0A1D5PZT4)	0.779	4	0.041	GCHFR
12	nei like DNA glycosylase 1 (F1NLM0)	0.790	2	0.046	NEIL1
13	isocitrate dehydrogenase 3 (NAD(+)) beta (A0A1D5PG36)	0.791	6	0.049	IDH3B
14	cell cycle progression 1 (A0A452J862)	0.795	2	0.049	CCPG1
15	caveolin 1 (A0M8T8)	0.795	4	0.011	CAV1
16	cadherin 13 (P33150)	0.796	1	0.048	CDH13
17	Uncharacterized protein (A0A3Q2UGY8)	0.796	3	0.031	novel gene
18	macrophage receptor with collagenous structure (F1NDC7)	0.801	4	0.007	MARCO
19	adaptor related protein complex 1 sigma 3 subunit (A0A3Q2TUZ1)	0.802	1	0.018	AP1S3
20	insulin like growth factor binding protein 7 (A0A1D5NUQ7)	0.806	2	0.043	IGFBP7
21	acyloxyacyl hydrolase (A0A1D5PNP0)	0.814	2	0.042	AOAH
22	hepatic lectin (E1C667)	0.816	8	0.004	LAD1
23	Cbl proto-oncogene (F1NXW5)	0.817	6	0.015	CBL
24	DENN domain containing 4A (A0A1D5PE26)	0.820	1	0.044	DENND4A
25	phosphodiesterase 6D (A0A1D5P2A3)	0.821	1	0.002	PDE6D
26	SH3 domain-containing protein (A0A3Q2U6C2)	0.826	2	0.037	novel gene
27	KIAA0100 (F1NMK5)	0.828	2	0.015	KIAA0100
28	fatty acid desaturase 2 (A6NAB8)	0.829	11	0.027	FADS2
29	Minichromosome maintenance complex component 2 (F1NB20)	1.204	7	0.027	MCM2
30	perilipin-4 (A0A1D5P6V5)	1.217	17	0.004	PLIN4
31	N-acetyltransferase 8 (GCN5-related, putative) (A0A3Q2UAZ8)	1.221	4	0.026	NAT8
32	protein phosphatase 1 regulatory subunit 12C (A0A3Q3ADX7)	1.225	1	0.029	PPP1R12C
33	cytosolic iron-sulfur assembly component 1 (A0A1D5PN77)	1.227	3	0.048	CIAO1
34	suppression of tumorigenicity 13 (colon carcinoma) (Hsp70 interacting protein) pseudogene 5 (F1NH21)	1.227	9	0.019	ST13P5
35	glutathione S-transferase theta 1 (P20135)	1.233	7	0.007	GSTT1
36	NAD(P)H quinone dehydrogenase 2 (R4GLI9)	1.260	7	0.005	NQO2
37	aldo-keto reductase family 1 member D1 (E1BU27)	1.264	16	0.016	AKR1D1
38	topoisomerase (DNA) II alpha (A0A1D5P9E6)	1.272	3	0.005	TOP2A
39	putative methyltransferase DDB_G0268948 (A0A1D5P5L5)	1.277	16	0.036	LOC107048987
40	ribonucleotide reductase regulatory subunit M2 (E1BXP4)	1.295	3	0.010	RRM2
41	glutathione S-transferase-like (A0A0A0MQ61)	1.357	10	0.016	LOC100859645
42	glutathione peroxidase 1 (R4GH86)	1.360	7	0.026	GPX1
43	glutathione S-transferase theta 1-like (E1BUB6)	1.368	5	0.024	GSTT1L
44	DnaJ heat shock protein family (Hsp40) member A4 (A0A1D5NYA8)	1.432	10	0.030	DNAJA4
45	heat shock protein family H (Hsp110) member 1 (E1BT08)	1.440	17	0.048	HSPH1
46	dnaJ homolog subfamily B member 1-like (A0A3Q2UAA1)	1.442	12	0.026	DNAJB1

approximately. The proteins of one unique peptide accounted for 14.9%, and others contained 2 ~ 118 unique peptides. The statistical data of protein characteristics are showed in S4 File. A total of 46 significant DEPs were detected in the CyCHS group compared with the control group for the liver samples, including 18 and 28 up- and down-regulated DEPs, respectively (Figure 1). The list of the 46 DEPs is showed in Table 1.

GO Annotations and KEGG Pathway Analysis

The GO enrichment analysis of DEPs was performed to investigate the biological processes (**BP**) related to CyCHS. We found that the enriched BP terms ($P < 0.05$) of the DEPs expressed in the liver were related to DNA metabolic process, oxidation-reduction process, oxidative stress and gluconeogenesis (Table 2). Based on the identified DEPs, two significantly enriched KEGG pathways appear to be involved in the liver response to CyCHS (Figure 1, Table 3). Five up-regulated DEPs were enriched in glutathione metabolism, namely glutathione peroxidase 1 (**GPX1**), glutathione S-transferase theta 1 (**GSTT1**), GSTT1-like (GSTT1L), glutathione S-transferase-like (LOC100859645), and ribonucleotide reductase regulatory subunit M2 (**RRM2**). The second enriched pathway was the TCA cycle, in which the isocitrate dehydrogenase 3 (NAD+) alpha (IDH3A), IDH3 beta (IDH3B) and phosphoenolpyruvate carboxykinase 1 (**PCK1**) were down-regulated.

To verify the DEPs identified by the LC-MS/MS analysis, eight DEPs were selected to determine their protein levels with PRM and expression levels with qRT-PCR. The PRM (Figure 2, S5 File) and qRT-PCR (Figure 3) results were consistent with the results of the LC-MS/MS analysis, supporting the proteomic data.

Table 2. The differentially abundant proteins involved in biological process of gene ontology.

Biological process terms	*P* value	Gene name
Oxidation-reduction process	0.0336	AKR1D1
		GPX1
		RRM2
		HAO2
		IDH3A
		IDH3B
Response to oxidative stress	0.0390	GPX1
DNA metabolic process	0.0059	MCM2
		TOP2A
		NEIL1
DNA topological change	0.0390	TOP2A
DNA replication initiation	0.0485	MCM2
Base-excision repair	0.0099	NEIL1
Gluconeogenesis	0.0294	PCK1

Abbreviations: AKR1D1: Aldo-keto reductase family 1 member D1; GPX1: Glutathione peroxidase 1; RRM2: Ribonucleotide reductase regulatory subunit M2; HAO2: Hydroxyacid oxidase 2; IDH3A: Isocitrate dehydrogenase 3 (NAD(+)) alpha; IDH3B: Isocitrate dehydrogenase 3 (NAD(+)) beta; MCM2: Minichromosome maintenance complex component 2; TOP2A: Topoisomerase (DNA) II alpha; NEIL1: Nei like DNA glycosylase 1; PCK1: Phosphoenolpyruvate carboxykinase 1.

Table 3. The differentially abundant proteins enriched in KEGG pathways.

KEGG pathways	*P* value	Description	Gene name
Glutathione metabolism	2.12 E-5	glutathione peroxidase 1	GPX1
		glutathione S-transferase theta 1	GSTT1
		glutathione S-transferase theta 1-like	GSTT1L
		glutathione S-transferase-like	LOC100859645
		ribonucleotide reductase regulatory subunit M2	RRM2
Citrate cycle (TCA cycle)	3.31 E-3	isocitrate dehydrogenase 3 (NAD(+)) alpha	IDH3A
		isocitrate dehydrogenase 3 (NAD(+)) beta	IDH3B
		phosphoenolpyruvate carboxykinase 1	PCK1

DISCUSSION

In this study, 46 DEPs were detected in YFC exposed to CyCHS using iTRAQ-based proteomic analyses. These DEPs were involved in DNA metabolic process, oxidative stress response, glutathione metabolism and TCA cycle pathway. In contrast, Tang et al. (2015) employed Sequential window acquisition of all theoretical mass spectra (**SWATH-MS**) analysis to investigate the response of broiler livers to HS and they identified 257 DEPs involved in the ERK signaling pathway, lipid and amino acid metabolism, and the cellular immune response. High temperatures have been linked to increased reactive oxygen species (ROS) production (Mujahid et al., 2005; Lin et al., 2006; Yang et al., 2010), oxidative stress, and an imbalance in antioxidants (Schiaffonati et al., 1990; Salo et al., 1991; Michiels et al., 2014), which together lead to oxidative damage, such as lipid peroxidation and DNA damage (Bruskov et al., 2002; Mujahid, 2007).

The liver is the main source of circulating glutathione (Lauterburg et al., 1983). The metabolism of glutathione is an important aspect of systemic activities to prevent ROS-induced cellular damage, which is a common sequela of HS (Wu et al., 2004; Lin et al., 2006). Oxidative stress may change the redox balance of reduced glutathione (GSH) and glutathione disulfide (GSSG) redox pairs, leading to changes in the expression of key enzymes such as detoxification, antioxidant defense, cell transformation, and the inflammatory response (Wu et al., 2004). The antioxidant enzymes play an important role in protecting cells from ROS-induced damage and the increased activity of these enzymes is a protective response to oxidative stress (Devi et al., 2000). Members of the glutathione peroxidase (GPX)

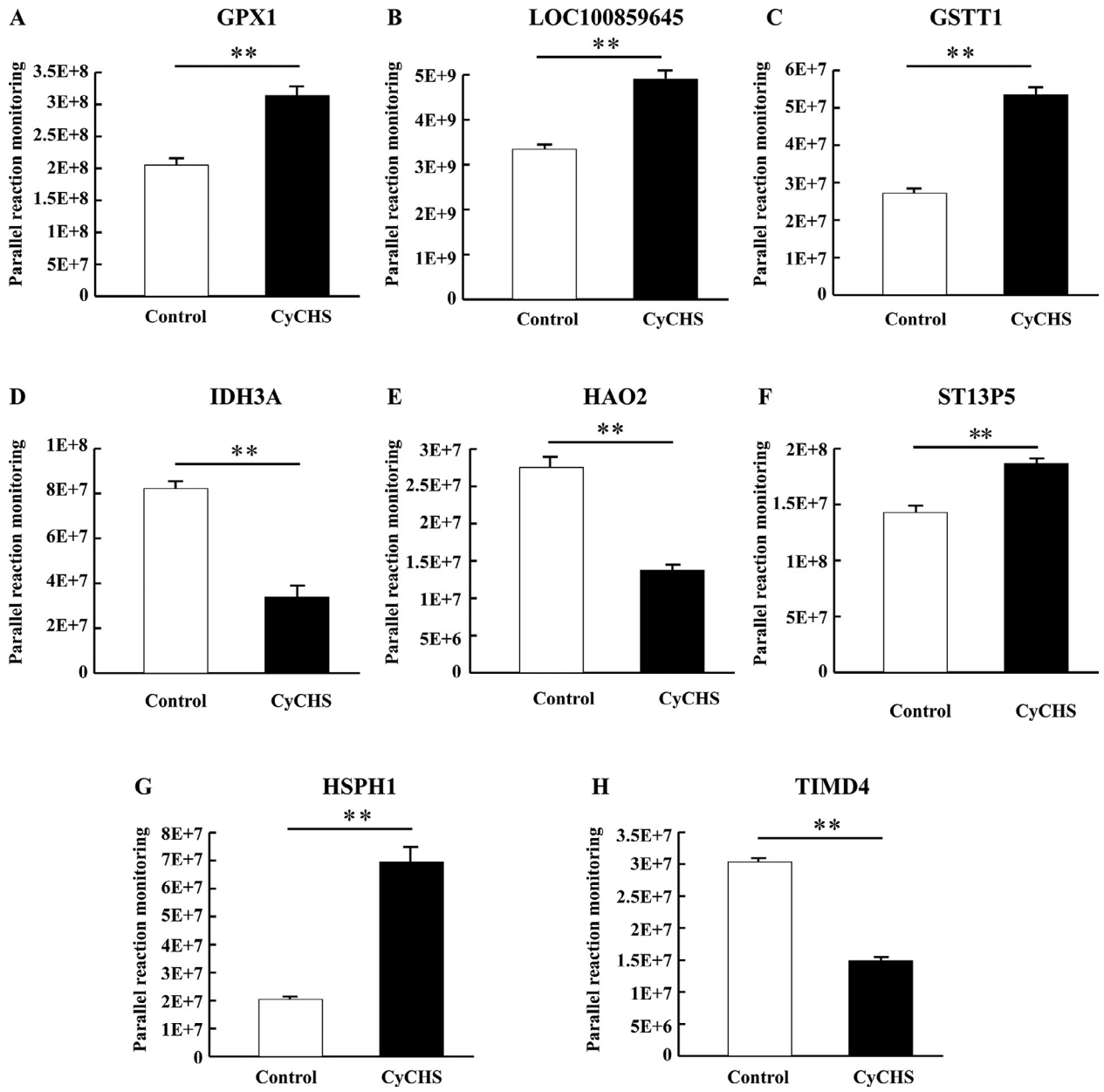

Figure 2. Verified the selected eight DEPs by Parallel reaction monitoring (PRM). PRM was used to determine the eight candidate proteins, and the results were consistent with those of LC-MS/MS analysis. Data are presented as mean ± SE (n = 9 per group). Control: control group (temperature constant maintained at 25 ± 1°C). CyCHS: cycle chronic heat stress group (38±1°C 8h/d, 7d). ** indicates significant difference ($P < 0.01$). A, B, C, D, E, F, G and H represent GPX1, LOC100859645, GSTT1, IDH3A, HAO2, ST13P5, HSPH1, and TIMD4, respectively.

family are important antioxidant enzymes, thanks to their ability to reduce hydroperoxides of polyunsaturated fatty acids, which counteracts the toxic effects of lipid peroxidation (Gattone et al., 2001; Basta et al., 2002; Jablonska et al., 2015). The GPX1 enzyme catalyzes the reaction between GSH and GSSG (Toppo et al., 2009). The glutathione S-transferase (GSTs), together with GPX1, protect cells from oxidative damage and allows them to adapt to oxidative stress (Hayes and Mclellan, 1999). GPX activity increased significantly in broilers exposed to HS (Ando et al., 1997; Altan et al., 2003). Chickens with increased glutathione circulation levels show less oxidative damage in response to HS compared with chickens exhibiting normal glutathione levels (Mahmoud and Edens, 2003). Studies examining acute HS showed that GSH/GSSG ratios decreased as a result of the increased oxidative damage (Hao et al., 2012). Under HS, total hepatic GSH levels were increased in male chickens (Willemsen et al., 2011) and it is possible that the liver has adapted by increasing GSH levels to compensate for periodic HS (Jastrebski et al., 2017), and increasing endogenous antioxidants (such as GSH) to adapt to chronic HS (Michiels et al., 2014). The HSP genes, which encode molecular chaperones, were shown to be up-regulated in response to HS-linked oxidative damage at the molecular level (Feder and Hofmann, 1999). A previous study showed that glutathione levels are regulated by HSP27, leading to change in the redox status of cells (Preville et al., 1996). Overexpression of GPX1 in mouse brain tissues reduced production of HSP70 in response to colonic temperature of mouse that were 42°C, which

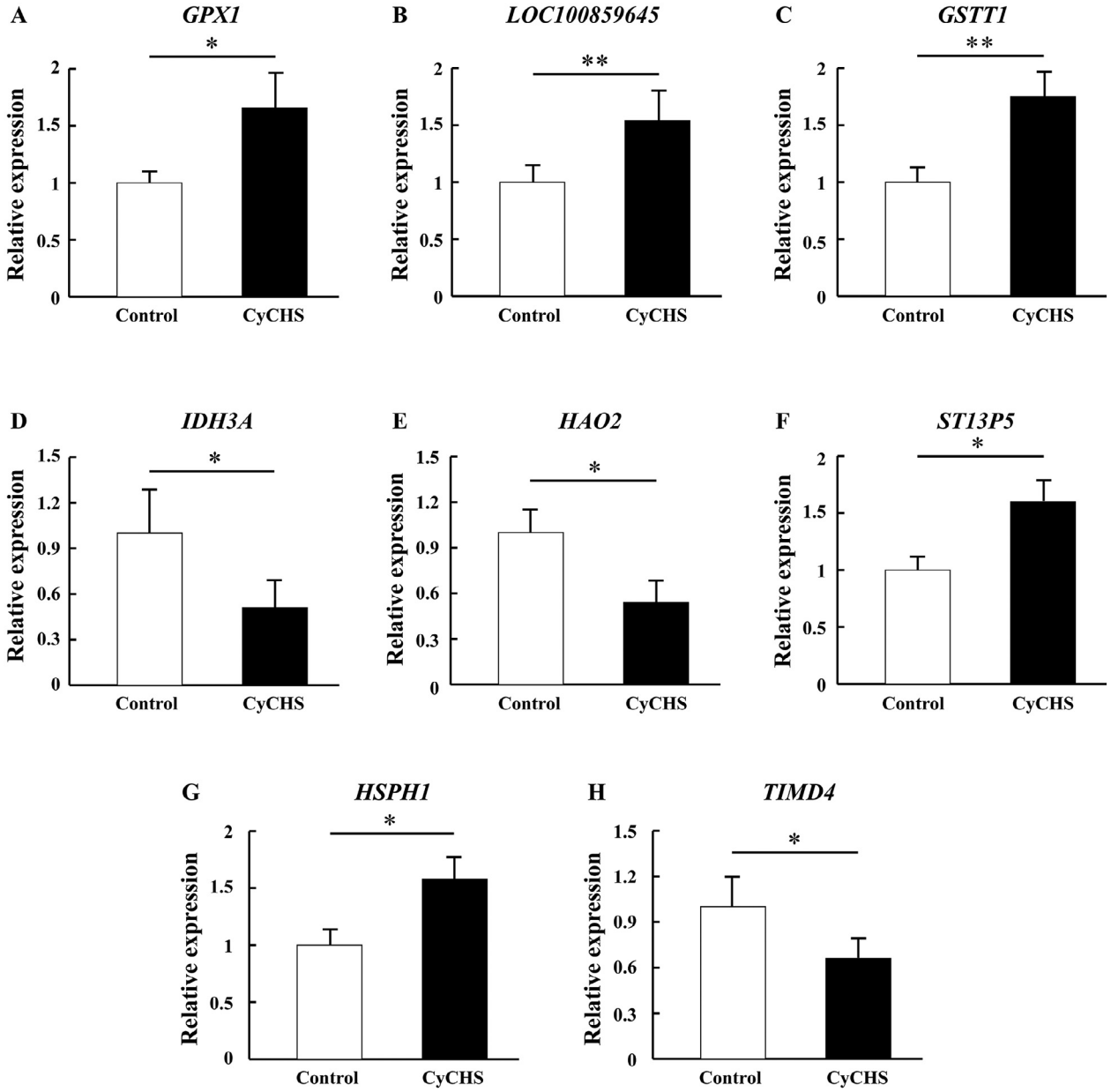

Figure 3. Verified the selected eight DEPs by real-time PCR. qRT-PCR was used to determine the eight candidate proteins, and the results were consistent with those of LC-MS / MS analysis. Data are presented as mean ± S.E (n = 9 per group). Control: control group (temperature constant maintained at 25 ± 1°C). CyCHS: cycle chronic heat stress group (38 ± 1°C 8 h/d, 7 d). * or ** indicate significant difference ($P < 0.05$ or 0.01, respectively). A, B, C, D, E, F, G and H represent *GPX1*, *LOC100859645*, *GSTT1*, *IDH3A*, *HAO2*, *ST13P5*, *HSPH1*, and *TIMD4*, respectively.

suggested that peroxides are directly involved in the cellular mechanisms of HSP70 induction and the regulation of body temperature (Mirochnitchenko et al., 1995). The stress tolerance of normal tissue was increased by HSPs or GSTs (Ban et al., 1996; Preville et al., 1996; Uozaki et al., 2015). Aldo-keto reductase (ARK), like GST and GPX, is part of an enzyme system that minimizes the by-products of oxidative stress (Hayes et al., 2005). The ARK family 1 member D1 (AKR1D1), which belongs to the ARK gene family, is mainly expressed in the liver (Iyer et al., 1990), and plays an essential role in bile acid biosynthesis (Russell and Setchell, 1992; Costanzo et al., 2009). The function of bile acid is to promote fat digestion and absorption (Máire et al., 2005; Reshetnyak, 2013), and increased bile acid levels in the diet were shown to improve the BWG and fat digestibility of broiler chickens (Parsaie et al., 2007; Alzawqari et al., 2016). Furthermore, a hypolipidemic phenotype was attributed to a reduction in duodenal bile acid concentration in broilers (Razdan et al., 1997). In this study, GPX1, GSTs (GSTT1, GSTT1L1, LOC100859645), AKR1D1, and HSPs (HSPH1, DNAJA4 and DNAJB1) were up-regulated in the liver of YFC, presumably to deal with the oxidative damage induced by CyCHS, and to improve the heat tolerance.

Among the metabolic pathways, the TCA cycle is a key route for managing the redox balance, biosynthetic and bioenergetic requirements of cells. The TCA cycle plays a pivotal role in cellular respiration and provides the transformation of various metabolites

(Yoshimi et al., 2016). In this study, IDH3A, IDH3B, and PCK1 were shown to be enriched in the TCA cycle using KEGG pathway analysis. The IDH3A and IDH3B form IDH3 complex (Mckenney and Levine, 2013), which plays the role of rate-limiting enzyme in TCA cycle and regulates the formation of NADH (Cairns and Mak, 2013) to product ATP (Hartong et al., 2008). HS has been shown to increase oxygen radicals, possibly by disrupting the electron transport assemblies of the mitochondrial membrane (Ando et al., 1997). Acute HS may induce the production of ROS in the liver tissue of broiler chickens by inhibiting mitochondrial respiration and ATP generation (Yang et al., 2010). Outside gluconeogenesis, the one of major pathways in which PCK1 participates is the conversion of amino acids to pyruvate for subsequent oxidation as acetyl-CoA in the TCA cycle (Yang et al., 2009). At high glucose, the activity of PCK1 gluconeogenesis pathway was reduced, which promoted the OAA into TCA as malate (Latorre et al., 2018). The total glucose production in the liver of PCK1 deficient mice decreased by 43%, suggesting the PCK1 involving the integration of energy metabolism in TCA cycle (Burgess et al., 2007). During HS, the heat energy release of animals was less than its produce (Ajakaiye et al., 2011) and led to impaired metabolism and death in broilers (Farrell and Swain, 1977; Hai et al., 2000).

HS-mediated generation of ROS may lead to oxidative damage of DNA (Bruskov et al., 2002). The family of minichromisome maintenance (**MCM**) proteins are essential for initiating the process of DNA replication and cell division (Bochman and Schwacha, 2009). MCMs are markers of proliferation that are highly active in proliferating cells and are down-regulated in senescent or differentiated cells (Freeman et al., 1999; Madine et al., 2000). Topoisomerase (DNA) II alpha (**TOP2A**) is an enzyme that controls topological changes of DNA, the segregation of newly duplicated chromosomes, aggregation, and chromosome formation. The inhibition of TOP2A activity results in the formation of bonds within the DNA chains, which leads to the obstruction of transcription and translation (Alexander, 2009). Previous studies have reported that nei like DNA glycosylase 1 (NEIL1) is regulated by the cell cycle, with expression levels peaking during S/G2 (Hazra and Mitra, 2006). NEIL1 also plays a role in DNA repair and coordination related to DNA replication, during active cell division (Albelazi et al., 2019). NEIL1 deficiency causes metabolic syndrome in mice, which suffer from a combination of severe obesity, dyslipidemia, and fatty liver disease (Vartanian et al., 2006). In this study, the expression of MCM2, TOP2A, and NEIL1 in the livers of YFC was down-regulated, which might have been the result of cell death caused by CyCHS.

CONCLUSIONS

Our quantitative proteomic data has expanded the known proteome coverage of liver tissue in YFC and provides new insights for the self-regulation mechanisms of YFC in response to CyCHS. Using iTRAQ analysis, 46 DEPs were detected to be involved in the CyCHS response of the YFC liver. The up-regulation of GPX1, GSTT1, GSTT1L, AKR1D1, and LOC100859645 in the glutathione metabolism pathway likely reflects an attempt to deal with oxidative damage by CyCHS, and improve the heat tolerance of the YFC. The down-regulation of IDH3A, IDH3B, and PCK1 in the TCA cycle pathway is probably to cope with the balance of heat production and dissipation during CyCHS in order to adapt to high temperature environments. Our results suggest that the liver of YFCs might activate anti-oxidants response and energy metabolism molecular mechanism of response to CyCHS, and provide a foundation for future studies of the functional genes involved in the HS and strategies for improving the negative effects of thermal environment on poultry productivity and welfare.

ACKNOWLEDGEMENTS

The authors would like to thank Guangdong YingFu agricultural Co., Ltd. for providing the experimental animals and sites.

DISCLSOURES

The authors certify they have no conflicting interests regarding the material discussed in the manuscript.

SUPPLEMENTARY MATERIALS

Supplementary material associated with this article can be found in the online version at doi:10.1016/j.psj.2021.101111.

REFERENCES

Ajakaiye, J. J., A. Perez-Bello, and A. Mollineda-Trujillo. 2011. Impact of heat stress on egg quality in layer hens supplemented with l-ascorbic acid and dl-tocopherol acetate. Vet. Arh. 81:119–132.

Akbarian, A., J. Michiels, J. Degroote, M. Majdeddin, A. Golian, and S. De Smet. 2016. Association between heat stress and oxidative stress in poultry; mitochondrial dysfunction and dietary interventions with phytochemicals. J. Anim. Sci. Biotechnol. 71:1–14.

Albelazi, M. S., P. R. Martin, S. Mohammed, L. Mutti, J. L. Parsons, and R. H. Elder. 2019. The biochemical role of the human NEIL1 and NEIL3 DNA glycosylases on model DNA replication forks. Genes. 10:315–326.

Alexander, V. 2009. Theoretical models of DNA topology simplification by type IIA DNA topoisomerases. Nucleic Acids Res. 10:3125–3133.

Altan, Ö., A. Pabuçcuoğlu, A. Altan, S. Konyalioğlu, and H. Bayraktar. 2003. Effect of heat stress on oxidative stress, lipid peroxidation and some stress parameters in broilers. Br. Poult. Sci. 44:545–550.

Alzawqari, M. H., H. H. Al-Baadani, I. B. Alhidary, A. N. Al-Owaimer, and A. M. Abudabos. 2016. Effect of taurine and bile acid supplementation and their interaction on performance, serum components, ileal viscosity and carcass characteristics of broiler chickens. South Afr. J. Anim. Sci. 46:448–457.

An, K., L. Fang, R. Luo, D. Wang, L. Xie, J. Yang, H. Chen, and S. Xiao. 2014. Quantitative proteomic analysis rReveals that

transmissible gastroenteritis virus (TGEV) activates JAK-STAT1 signaling pathway. J. Proteome Res. 13:5376–5390.
Ando, M., K. Katagiri, S. Yamamoto, K. Wakamatsu, I. Kawahara, S. Asanuma, M. Usuda, and K. Sasaki. 1997. Age-related effects of heat stress on protective enzymes for peroxides and microsomal monooxygenase in rat liver. Environ. Health Perspect. 105:726–733.
Azad, K. M. A., M. Kikusato, A. M. Hoque, and M. Toyomizu. 2010. Effect of chronic heat htress on performance and oxidative damage in different strains of chickens. J. Poult. Sci. 47:333–337.
Ban, N., Y. Takahashi, T. Takayama, T. Kura, S. Sakamaki, and Y. Niitsu. 1996. Transfection of glutathione s-transferase (GST)-π antisense complementary DNA increases the sensitivity of a colon cancer cell line to adriamycin, cisplatin, melphalan, and etoposide. Cancer Res. 56:3577–3582.
Basta, G., G. Lazzerini, M. Massaro, T. Simoncini, P. Tanganelli, C. Fu, T. Kislinger, D. M. Stern, A. M. Schmidt, and R. De Caterina. 2002. Advanced glycation end products activate endothelium through signal-transduction receptor RAGE a mechanism for amplification of inflammatory responses. Circulation. 105:816–822.
Blikslager, A. T., N. A. White II, J. N. Moore, and T. S. Mair. 2017. The equine acute abdomen. Pages 55−57 in Liver Function. T. S. Mair, ed. 3rd ed. John Wiley & Sons Inc., Hoboken, NJ.
Bochman, M. L., and A. Schwacha 2009. The mcm complex: unwinding the mechanism of a replicative helicase. Microbiol. Mol. Biol. Rev. 73:652–683.
Bruskov, V. I., L. V. Malakhova, Z. K. Masalimov, and A. V. Chernikov. 2002. Heat-induced formation of reactive oxygen species and 8-oxoguanine, a biomarker of damage to DNA. Nucleic Acids Res. 30:1354–1363.
Burgess, S. C., T. He, Z. Yan, J. Lindner, D. Sherry, C. R. Malloy, J. D. Browning, and M. A. Magnuson. 2007. Cytosolic phosphoenolpyruvate carboxykinase does not solely control the rate of hepatic gluconeogenesis in the intact mouse liver. Cell Metab. 5:313–320.
Cahaner, A., and F. Leenstra 1992. Effects of high temperature on growth and efficiency of male and female broilers from lines selected for high weight gain, favorable feed conversion, and high or low fat content. Poult. Sci. 71:1237–1250.
Cairns, R. A., and T. W. Mak 2013. Oncogenic isocitrate dehydrogenase mutations: mechanisms, models, and clinical opportunities. Cancer Discov. 3:730–741.
Coble, D. J., D. Fleming, M. E. Persia, C. Ashwell, M. F. Rothschild, C. J. Schmidt, and S. J. Lamont. 2014. RNA-seq analysis of broiler liver transcriptome reveals novel responses to high ambient temperature. BMC Genomics. 15:1084.
Costanzo, L. D., J. E. Drury, D. W. Christianson, and T. M. Penning. 2009. Structure and catalytic mechanism of human steroid 5β-reductase (AKR1D1). Mol. Cell. Endocrinol. 301:191–198.
Deng, X., B. Du, F. Zhu, Y. Gao, and J. Li. 2020. Proteomic analysis of aspergillus niger 3.316 under heat stress. MicrobiologyOpen. 9: e1012.
Devi, G. S., M. H. Prasad, I. Saraswathi, D. Raghu, D. N. Rao, and P. Reddy. 2000. Free radicals antioxidant enzymes and lipid peroxidation in different types of leukemias. Clin. Chim. Acta. 293:53–62.
Diz, A. P., M. Truebano, and D. O. F. Skibinski. 2009. The consequences of sample pooling in proteomics: an empirical study. Electrophoresis. 30:2967–2975.
Farrell, D. J., and S. Swain 1977. Effects of temperature treatments on the energy and nitrogen metabolism of fed chickens. Brit. Poult. Sci. 18:735–748.
Feder, M. E., and G. E. Hofmann 1999. Heat shock proteins, molecular chaperones, and the stress response: evolutionary and ecological physiology. Annu. Rev. Physiol. 61:243–282.
Freeman, A., L. S. Morris, A. D. Mills, K. Stoeber, R. A. Laskey, G. H. Williams, and N. Coleman. 1999. Minichromosome maintenance proteins as biological markers of dysplasia and malignancy. Clin. Cancer Res. 5:2121–2132.
Gattone, M., L. Iacoviello, M. Colombo, A. D. Castelnuovo, F. Soffiantino, A. Gramoni, D. Picco, M. Benedetta Donati, and P. Giannuzzi. 2001. Chlamydia pneumoniae and cytomegalovirus seropositivity, inflammatory markers, and the risk of myocardial infarction at a young age. Am. Heart J. 142:633–640.
Hai, L., D. Rong, and Z. Y. Zhang. 2000. The effect of thermal environment on the digestion of broilers. J. Anim. Physiol. Anim. Nutr. 83:57–64.
Hao, Y., X. H. Gu, and X. L. Wang. 2012. Overexpression of heat shock protein 70 and its relationship to intestine under acute heat stress in broilers: 1. Intestinal structure and digestive function. Poult. Sci. 91:781–789.
Hartong, D. T., M. Dange, T. L. Mcgee, E. L. Berson, T. P. Dryja, and R. F. Colman. 2008. Insights from retinitis pigmentosa into the roles of isocitrate dehydrogenases in the Krebs cycle. Nature Genet. 40:1230–1234.
Hayes, J. D., J. U. Flanagan, and I. R. Jowsey. 2005. Glutathione transferases. Annu. Rev. Pharmacol. Toxocol. 45:51–88.
Hayes, J. D., and L. I. Mclellan 1999. Glutathione and glutathione-dependent enzymes represent a co-ordinately regulated defence against oxidative stress. Free Radic. Res. 31:273–300.
Hazra, T. K., and S. Mitra 2006. Purification and characterization of NEIL1 and NEIL2, members of a distinct family of mammalian DNA glycosylases for repair of oxidized bases. Methods Enzymol. 408:33–48.
Iyer, R., J. M. Binstock, I. S. Schwartz, G. G. Gordon, B. I. Weinstein, and A. L. Southren. 1990. Human hepatic cortisol reductase activities: enzymatic properties and substrate specificities of cytosolic cortisol Δ4-5β-reductase and dihydrocortisol-3α-oxidoreductase(s). Steroids. 55:495–500.
Jablonska, E., J. Gromadzinska, B. Peplonska, W. Fendler, E. Reszka, M. B. Krol, E. Wieczorek, A. Bukowska, P. Gresner, M. Galicki, O. Z. Quispe, Z. Morawiec, and W. Wasowicz. 2015. Lipid peroxidation and glutathione peroxidase activity relationship in breast cancer depends on functional polymorphism of GPX1. BMC Cancer. 15:657.
Jastrebski, S. F., S. J. Lamont, and C. J. Schmidt. 2017. Chicken hepatic response to chronic heat stress using integrated transcriptome and metabolome analysis. PLoS One. 12:e0181900.
Jianzhen, H., M. Haitian, Y. Liming, and Z. Sixiang. 2007. Developmental changes of protein profiles in the embryonic sanhuang chicken liver. J. Vet. Med. A. Physiol. Pathol. Clin. Med. 54:464–469.
La, Y., J. Tang, X. Guo, L. Zhang, S. Gan, X. Zhang, J. Zhang, W. Hu, and M Chu. 2020. Proteomic analysis of sheep uterus reveals its role in prolificacy. J. Proteomics. 210:103526.
Lan, X., J. C. F. Hsieh, C. J. Schmidt, Q. Zhu, and S. J. Lamont. 2016. Liver transcriptome response to hyperthermic stress in three distinct chicken lines. BMC Genomics. 17:955.
Latorre, P., J. Baeza, E. A. Armstrong, R. Hurtado-Guerrero, F. Corzana, L. E. Wu, D. A. Sinclair, P. L. Buesa, J. Carrodeguas, and J. M. Denu. 2018. Dynamic acetylation of phosphoenolpyruvate carboxykinase toggles enzyme activity between gluconeogenic and anaplerotic reactions. Mol. Cell. 71:718–732.
Lauterburg, B. H., J. D. Adams, and J. R. Mitchell. 1983. Hepatic glutathione homeostasis in the rat: Efflux accounts for glutathione turnover. Hepatology. 4:586–590.
Lin, H., E. Decuypere, and J. Buyse. 2006. Acute heat stress induces oxidative stress in broiler chickens. Comp. Biochem. Physiol. A-Mol. Integr. Physiol. 144:11–17.
Livak, K. J., and T. D. Schmittgen 2001. Analysis of relative gene expression data using real-time quantitative PCR and the 2(-delta delta C(T)) method. Methods. 25:402–408.
Luo, J, A. Zheng, K. Meng, W. Chang, Y. Bai, K. Li, H. Cai, G. Liu, and B. Yao. 2013. Proteome changes in the intestinal mucosa of broiler (Gallus gallus) activated by probiotic enterococcus faecium. J. Proteomics. 91:226–241.
Maclean, B., D. M. Tomazela, N. J. Shulman, M. C. Chambers, G. L. Finney, B. Frewen, R. Kern, D. L. Tabb, D. C. Liebler, and M. J. Maccoss. 2010. Skyline: an open source document editor for creating and analyzing targeted proteomics experiments. Bioinformatics. 26:966–968.
Madine, M. A., M. Swietlik, C. Pelizon, P. Romanowski, A. D. Mills, and R. A. Laskey. 2000. The roles of the MCM, ORC, and cdc6 proteins in determining the replication competence of chromatin in quiescent cells. J. Struct. Biol. 129:198–210.
Mahmoud, K. Z., and F. W. Edens 2003. Influence of selenium sources on age-related and mild heat stress-related changes of blood and

liver glutathione redox cycle in broiler chickens (Gallus domesticus). Comp. Biochem. Physiol. B. Biochem. Mol. Biol. 136:921–934.
Mckenney, A. S., and R. L. Levine 2013. Isocitrate dehydrogenase mutations in leukemia. J. Clin. Invest. 123:3672–3677.
Michiels, J., M. M. Tagliabue, A. Akbarian, A. Ovyn, and S. D. Smet. 2014. Oxidative status, meat quality and fatty acid profile of broiler chickens reared under free-range and severely feed-restricted conditions compared with conventional indoor rearing. Avian Biol. Res. 7:74–82.
Mirochnitchenko, O., U. Palnitkar, M. A. Philbert, and M. Inouye. 1995. Thermosensitive phenotype of transgenic mice overproducing human glutathione peroxidases. Proc. Natl. Acad. Sci. 92:8120–8124.
Mujahid, A. 2007. Acute heat stress induces oxidative stress and decreases adaptation in young white leghorn cockerels by downregulation of avian uncoupling protein. Poult. Sci. 86:364–371.
Mujahid, A., Y. Akiba, and M. Toyomizu. 2005. Superoxide radical production in chicken skeletal muscle induced by acute heat stress. Poult. Sci. 84:307–314.
National Reasearch Council. 1994. Nuteient Requirements of Poultry. 9th rev. Natl. Acad. Press, Washington, DC.
Parsaie, S., F. Shariatmadari, M. J. Zamiri, and K. Khajeh. 2007. Influence of wheat-based diets supplemented with xylanase, bile acid and antibiotics on performance, digestive tract measurements and gut morphology of broilers compared with a maize-based diet. Br. Poult. Sci. 48:594–600.
Philip, J., B. David, H. Y. Chang, F. Matthew, W. Li, M. Craig, M. Hamish, M. John, M. Alex, and N. Gift. 2014. InterProScan 5: genome-scale protein function classification. Bioinformatics. 9:1236–1240.
Preville, X., P. Mehlen, N. Fabre-Jonca, S. Chaufour, C. Kretzremy, M. R. Michel, and A. Arrigo. 1996. Biochemical and immunofluorescence analysis of the constitutively expressed HSP27 stress protein in monkey CV-1 cells. J. Biosci. 21:221–234.
Quinteiro-Filho, W. M., A. Ribeiro, V. Ferraz-de-Paula, M. L. Pinheiro, M. Sakai, L. R. M. Sa, A. J. P. Ferreira, and J. Palermo-Neto. 2010. Heat stress impairs performance parameters, induces intestinal injury, and decreases macrophage activity in broiler chickens. Poult. Sci. 89:1905–1914.
Razdan, A., D. Pettersson, and J. Pettersson. 1997. Broiler chicken body weights, feed intakes, plasma lipid and small-intestinal bile acid concentrations in response to feeding of chitosan and pectin. Br. J. Nutr. 78:283–291.
Ren, W., X. Hou, Y. Wang, W. Badgery, X. Li, Y. Ding, H. Guo, Z. Wu, N. Hu, L. Hu, L. Kong, C. Chang, C. Jiang, and J. Zhang. 2017. Overgrazing induces alterations in the hepatic proteome of sheep (ovis aries): an itraq-based quantitative proteomic analysis. Proteome Sci. 15:2.
Reshetnyak, V. I. 2013. Physiological and molecular biochemical mechanisms of bile formation. World J. Gastroenterol. 19:7341–7360.
Russell, D. W., and K. D. R. Setchell 1992. Bile acid biosynthesis. Biochemistry. 31:4737–4749.
Salo, D. C., C. M. Donovan, and K. J. A. Davies. 1991. HSP70 and other possible heat shock or oxidative stress proteins are induced in skeletal muscle, heart, and liver during exercise. Free Radic. Biol. Med. 11:239–246.
Schiaffonati, L., E. Rappocciolo, L. Tacchini, G. Cairo, and A. Bernellizazzera. 1990. Reprogramming of gene expression in postischemic rat liver: induction of proto-oncogenes and hsp 70 gene family. J. Cell. Physiol. 143:79–87.
Tang, X., Q. Meng, J. Gao, S. Zhang, H. Zhang, and M. Zhang. 2015. Label-free quantitative analysis of changes in broiler liver proteins under heat stress using SWATH-MS technology. Sci. Rep. 5:15119.
Toppo, S., L. Flohe, F. Ursini, S. Vanin, and M. Maiorino. 2009. Catalytic mechanisms and specificities of glutathione peroxidases: Variations of a basic scheme. Biochim. Biophys. Acta. 1790:1486–1500.
Uozaki, H., H. Horiuchi, T. Ishida, T. Iijima, T. Imamura, and R. Machinami. 2015. Overexpression of resistance-related proteins (metallothioneins, glutathione-S-transferase pi, heat shock protein 27, and lung resistance-related protein) in osteosarcoma. Relationship with poor prognosis. Cancer. 79:2336–2344.
Van Goor, A., K. J. Bolek, C. M. Ashwell, M. E. Persia, M. F. Rothschild, C. J. Schmidt, and S. J. Lamont. 2015. Identification of quantitative trait loci for body temperature, body weight, breast yield, and digestibility in an advanced intercross line of chickens under heat stress. Genet. Sel. Evol. 47:96.
Vartanian, V., B. Lowell, I. G. Minko, T. G. Wood, J. D. Ceci, S. George, S. W. Ballinger, C. L. Corless, A. K. Mccullough, and R. S. Lloyd. 2006. The metabolic syndrome resulting from a knockout of the NEIL1 DNA glycosylase. Proc. Natl. Acad. Sci. 103:1864–1869.
Willemsen, H., Q. Swennen, N. Everaert, P. Geraert, Y. Mercier, A. Stinckens, E. Decuypere, and J. Buyse. 2011. Effects of dietary supplementation of methionine and its hydroxy analog DL-2-hydroxy-4-methylthiobutanoic acid on growth performance, plasma hormone levels, and the redox status of broiler chickens exposed to high temperatures. Poult. Sci. 90:2311–2320.
Wu, G., Y. Z. Fang, S. Yang, J. R. Lupton, and N. D. Turner. 2004. Glutathione Metabolism and Its Implications for Health. J. Nutr. 134:489–492.
Yang, J., S. C. Kalhan, and R. W. Hanson. 2009. What is the metabolic role of phosphoenolpyruvate carboxykinase. J. Biol. Chem. 284:27025–27029.
Yang, L., G. Y. Tan, Y. Q. Fu, J. H. Feng, and M. H. Zhang. 2010. Effects of acute heat stress and subsequent stress removal on function of hepatic mitochondrial respiration, ROS production and lipid peroxidation in broiler chickens. Comp. Biochem. Phys. C. 151:204–208.
Yoshimi, N., T. Futamura, S. E. Bergen, Y. Iwayama, T. Ishima, C. Sellgren, C. J. Ekman, J. Jakobsson, E. Palsson, Y. Ohgi, T. Yoshikawa, M. Landen, and K. Hashimoto. 2016. Cerebrospinal fluid metabolomics identifies a key role of isocitrate dehydrogenase in bipolar disorder: evidence in support of mitochondrial dysfunction hypothesis. Mol. Psychiatry. 21:1504–1510.
Zeng, T., X. Jiang, J. Li, D. Wanf, G. Li, and G. Wang. 2013. Comparative proteomic analysis of the hepatic response to heat stress in muscovy and pekin ducks: insight into thermal tolerance related to energy metabolism. PLoS One 8:e76917.
Zhang, J., C. J. Schmidt, and S. J. Lamont. 2017. Transcriptome analysis reveals potential mechanisms underlying differential heart development in fast-and slow-growing broilers under heat stress. Bmc Genomics. 18:295.
Zhang, Q., Y. K. Luo, B. H. Zhang, Y. Z. Chan, L. L. Huang, Y. Wang, J. M. Liang, and X. Q. Zhang. 2020. RNA-Seq study of hepatic response of yellow-feather chickens to acute heat stress. Ann. Anim. Sci. 20:55–69.
Zhang, Q., B. Zhang, and Y. Luo. 2019. Cardiac transcriptome study of the effect of heat stress in yellow-feather broilers. Ital. J. Anim. Sci. 18:971–975.